53rd IEEE Conference on Decision and Control
December 15-17, 2014. Los Angeles, California, USA

Aspects in Inferential Iterative Learning Control: A 2D Systems Analysis

Joost Bolder, Tom Oomen, and Maarten Steinbuch

Abstract— **Increasing performance requirements lead to a situation where performance variables need to be explicitly distinguished from measured variables. The performance variables are not available for feedback. Instead, they are often available after a task. This enables the application of batch-to-batch control strategies such as Iterative Learning Control (ILC) to the performance variables. The aim of this paper is to reveal potential problems in combining ILC and feedback control for this scenario, and to propose a solution. The time-trial dynamics of a common ILC algorithm with dynamic learning filters are cast into discrete linear repetitive processes, a class of 2D systems. Appropriate 2D stability notions are connected to well-known conditions on the ILC algorithm. The analysis reveals that there are important cases where the ILC and feedback combination is not stable in a 2D sense. A solution to deal with such cases is proposed. The analysis is supported with a simulation example of medium positioning drive in a printing system.**

I. Introduction

Increasing performance requirements on systems demand an explicit distinction between measured variables and performance variables. Performance variables may not be available for real-time feedback control due to computational constraints, due to physical limitations in sensor placement, or due to delays in acquiring measurements. Examples include heat exchangers [20], printing systems [3], motion systems [16], [17], and wafers stages [18]. Still, the performance variables are typically available after a task is completed.

Since the performance variables are available offline, batch-to-batch control strategies such as Iterative Learning Control (ILC) [5], [6], [10] can be used to improve performance. In ILC, the control signal is updated trial-to-trial using measurement data of previous trials, often achieving excellent performance. Traditionally, ILC is applied to the measured variables [11], [14], [19], [23]. Recently, ILC has been extended to deal with the inferential control situation [4], [12], [26]. In [4, Figure 9] it was demonstrated that the combination of ILC with feedback control can lead to the undesired case where the command signals of the feedback controller and ILC grow unbounded with opposite signs.

Although ILC is potentially promising for the mentioned inferential control applications, a formal analysis of the stability aspects is lacking. The main result of the present paper is the in-depth analysis of inferential ILC schemes. The approach is to cast time-trial dynamics of a commonly used ILC algorithm [5] into a linear repetitive process, a class of 2D systems [8], [22]. Appropriate 2D stability notions are connected to commonly known conditions on the ILC algorithm. An important motivation for using 2D systems theory for ILC design is usually the joint synthesis of ILC and feedback controllers [21], which contrasts with the two-stage design procedure as elaborated on in [5], where first the feedback controller and then the ILC is designed. In this paper, the motivation for using 2D systems mainly stems from the observation that the source of the unstable behavior reported in [4] is the interplay of the feedback controller with the ILC. The 2D framework enables the formal analysis of this situation, in contrast to the finite-time framework in [4].

This paper is organized as follows. First, the problem definition and contributions are presented in Section II. In Section III, a commonly known ILC algorithm with dynamic learning filters is cast into a discrete linear repetitive process and stability notions from 2D systems are connected with well-known conditions on the ILC algorithm and system. In Section IV, a parallel inferential ILC structure is investigated and a solution to stability problems is proposed. The results are supported with a simulation example in Section V. Finally, the conclusion is presented in Section VI.

II. Problem definition and main contributions

In the considered inferential ILC situation, the feedback controller only has access to the measured variables. The performance variables are assumed available after a task and are used for ILC. In [4, Figure 9] it was demonstrated that this combination of ILC with feedback control can lead to the undesired situation where the command signals of the feedback controller and ILC increase unbounded. The finite-time framework that is used in [4] is not suited for analyzing the stability aspects of the interplay between the feedback controller and the ILC. Therefore, this paper aims to formally analyze inferential ILC from a 2D system-theoretic perspective. The main contributions of this paper are as follows:

1) the 2D-stability notion of stability along the pass is connected to the commonly known frequency domain convergence condition of the ILC algorithm [15],
2) the analysis of stability along the pass and the signal characteristics for inferential ILC configurations, revealing potential stability hazards,
3) The results are illustrated with a simulation example.

The authors are with the Eindhoven University of Technology, Dept. of Mechanical Engineering, Control Systems Technology group, P.O. Box 513, 5600 MB Eindhoven, The Netherlands, j.j.bolder@tue.nl

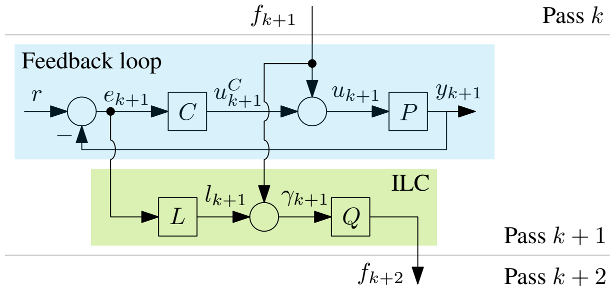

Fig. 1: Standard ILC with feedback control in a parallel configuration.

III. Linear repetitive process framework for ILC with dynamic L and Q

This section contains contribution 1, mentioned in Section II. The ILC framework used in this paper is presented in Fig. 1. The structure consists of a feedback loop with feedforward, where the feedforward is the command signal of the ILC. The system $P(z)$, controller, $C(z)$, learning filter $L(z)$, and robustness filter $Q(z)$ are assumed single-input and single-output and causal. The system $P(z)$ is assumed strictly proper. After a trial (or pass) k, the feedforward is updated with the ILC algorithm:

$$f_{k+1} = Q\left(f_k + Le_k\right), \tag{1}$$

with e_k is the tracking error and f_k the feedfoward. The time-index is p and the trial index (also called pass index) is denoted as k. State space realizations for the systems in Fig. 1 are given by:

$$\begin{aligned}
P:&\quad \begin{array}{rcl} x^P_{k+1}(p+1) &=& A^P x^P_{k+1}(p) + B^P u_{k+1}(p),\\ y_{k+1}(p) &=& C^P x^P_{k+1}(p),\end{array}\\
C:&\quad \begin{array}{rcl} x^C_{k+1}(p+1) &=& A^C x^C_{k+1}(p) + B^C e_{k+1}(p),\\ u^C_{k+1}(p) &=& C^C x^C_{k+1}(p) + D^C e_{k+1}(p),\end{array}\\
L:&\quad \begin{array}{rcl} x^L_{k+1}(p+1) &=& A^L x^L_{k+1}(p) + B^L e_{k+1}(p),\\ l_{k+1}(p) &=& C^L x^L_{k+1}(p) + D^L e_{k+1}(p),\end{array}\\
Q:&\quad \begin{array}{rcl} x^Q_{k+1}(p+1) &=& A^Q x^Q_{k+1}(p) + B^Q \gamma_{k+1}(p),\\ f_{k+2}(p) &=& C^Q x^Q_{k+1}(p) + D^Q \gamma_{k+1}(p),\end{array}
\end{aligned} \tag{2}$$

respectively, and are assumed minimal. Also,

$$\begin{aligned}
e_{k+1}(p) &= r(p) - y_{k+1}(p),\\
u_{k+1}(p) &= u^C_{k+1}(p) + f_{k+1}(p),\\
\gamma_{k+1}(p) &= f_k(p) + l_{k+1}(p),
\end{aligned} \tag{3}$$

see Fig. 1. The framework of Fig. 1 is cast into a discrete Linear Repetitive Process (dLRP) in the following lemma.

Lemma 1. *A dLRP representation of the control structure defined in* (2) *and* (3)*, see also Fig. 1, is given by:*

$$\begin{aligned}
\mathcal{X}_{k+1}(p+1) &= \mathcal{A}\mathcal{X}_{k+1}(p) + \mathcal{B}r(p) + \mathcal{B}_0\mathcal{Y}_k(p)\\
\mathcal{Y}_{k+1}(p) &= \mathcal{C}\mathcal{X}_{k+1}(p) + \mathcal{D}r(p) + \mathcal{D}_0\mathcal{Y}_k(p)
\end{aligned} \tag{4}$$

with the states defined as:

$$\mathcal{X}_{k+1}(p) = \begin{bmatrix} x^P_{k+1}(p)\\ x^C_{k+1}(p)\\ x^L_{k+1}(p)\\ x^Q_{k+1}(p)\end{bmatrix}, \quad \mathcal{Y}_{k+1}(p) = \begin{bmatrix} f_{k+2}(p)\end{bmatrix}.$$

The matrices $\mathcal{A}, \mathcal{B}, \mathcal{B}_0, \mathcal{C}, \mathcal{D}$, and $\mathcal{D}_0$ are given in (5)*. Here, p denotes the discrete-time, $k \geq 0$ is the pass index (or trial index), and α the pass length with $0 \leq p \leq \alpha - 1$. For a pass k, the state is denoted as $\mathcal{X}_k(p)$, the pass profile is denoted as $\mathcal{Y}_k(p)$, and the input is the reference $r(p)$, which is assumed pass-invariant. The initial conditions are assumed $\mathcal{X}_{k+1}(0) = 0$ and $\mathcal{Y}_0(p) = 0$.*

$$\begin{aligned}
\mathcal{A} &= \begin{bmatrix} A^P - B^P D^C C^P & B^P C^C & 0 & 0\\ -B^C C^P & A^C & 0 & 0\\ -B^L C^P & 0 & A^L & 0\\ -B^Q D^L C^P & 0 & B^Q C^L & A^Q \end{bmatrix}, \mathcal{B}_0 = \begin{bmatrix} B^P\\ 0\\ 0\\ B^Q\end{bmatrix},\\
\mathcal{B} &= \begin{bmatrix} B^P D^C\\ B^C\\ B^L\\ B^Q D^L\end{bmatrix}, \qquad \begin{array}{l} \mathcal{C} = \begin{bmatrix} -D^Q D^L C^P & 0 & D^Q C^L & C^Q\end{bmatrix},\\ \mathcal{D} = \begin{bmatrix} D^Q D^L\end{bmatrix}, \qquad \mathcal{D}_0 = \begin{bmatrix} D^Q \end{bmatrix}.\end{array}
\end{aligned} \tag{5}$$

Proof. Successive substitution of the output-equations and state-update equations from (2) in the interconnection equations in (3) yields the given representation, after suitable partitioning. □

Convergence of the feedforward signal f_k, stability of the feedback loop, and a stable interconnection of the feedback loop with the ILC are all essential properties for implementing an ILC algorithm. These properties are captured with the the notion of stability along the pass for dLRP's, see [2], [8, Section 3.4], and [22, Section 2.2]. Stability along the pass demands that i. the pass profile $\mathcal{Y}_k$ converges to a limit profile $\mathcal{Y}_\infty$ when $k \to \infty$, ii. the time-domain dynamics (p-direction, for a given k) are asymptotically stable, and iii. each frequency component of the initial pass profile is attenuated from pass-to-pass [22].

Lemma 2. *Suppose in* (4)*, that the pair $\{\mathcal{A}, \mathcal{B}_0\}$ is controllable and that the pair $\{\mathcal{C}, \mathcal{A}\}$ is observable. The dLRP in* (4) *is stable along the pass if, and only if, the following three conditions hold.*

1) *$\rho(\mathcal{D}_0) < 1$, the dLRP is asymptotically stable, here $\rho(\mathcal{D}_0)$ is the spectral radius of matrix $\mathcal{D}_0$.*
2) *$\rho(\mathcal{A}) < 1$, the time-domain dynamics with $\mathcal{Y}_k = 0$ are asymptotically stable.*
3) *Let $G(z) = \mathcal{C}(zI - \mathcal{A})^{-1}\mathcal{B}_0 + \mathcal{D}_0$, then $\rho(G(z)) < 1, \forall |z| = 1,\ z \in \mathbb{C}$.*

Proof. See [22, Theorem 2.2.9]. □

The following theorem establishes conditions for stability along the pass for the ILC algorithm in (1).

Theorem 3. *Given the dLRP in* (4) *with $\mathcal{A}, \mathcal{B}, \mathcal{B}_\mathbf{0}, \mathcal{C}, \mathcal{D}$, and $\mathcal{D}_\mathbf{0}$ given in* (5)*. The dLRP is stable along the pass, see Lemma 2, if the following conditions are satisfied:*
I. $\rho(D^Q) < 1$,
II. *the feedback interconnection of C and P is internally*

stable, $\rho(A^L) < 1$, *and* $\rho(A^Q) < 1$,
III. *the following holds:*

$$|Q(z)(I - L(z)P(z)S(z))| < 1, \forall |z| = 1, \tag{6}$$

with $S(z) = 1/(1 + CP)$ *the sensitivity, and* $z \in \mathbb{C}$,
IV. *consider the following state-space realization of* $Q(1 - PSL)$ *that corresponds to* (2)*, with interconnection equations* (3)*,* $r(p) = 0$*, input* f_{k+1}*, and output* f_{k+2}*:*

$$\begin{aligned} \mathbf{x}(p+1) &= \mathcal{A}\mathbf{x}(p) + \mathcal{B}_0 f_{k+1}(p), \\ f_{k+2}(p) &= \mathcal{C}\mathbf{x}(p) + \mathcal{D}_0 f_{k+1}(p), \end{aligned} \tag{7}$$

matrices $\mathcal{A}, \mathcal{B}_0, \mathcal{C}$*, and* $\mathcal{D}_0$ *are given in* (5)*. The state space realization in* (7) *is minimal.*

Proof. The proof establishes the equivalence of the conditions provided in this theorem with the conditions that are required for stability along the pass in Lemma 2.
I. Since $\mathcal{D}_0 = D^Q$, $\rho(\mathcal{D}_0) < 1 \Leftrightarrow \rho(D^Q) < 1$.
II. Consider the lower triangular structure of $\mathcal{A}$, see (5). The set of eigenvalues of $\mathcal{A}$ is given by $\lambda(\mathcal{A}) = \{\lambda(A^{CP}), \lambda(A^L), \lambda(A^Q)\}$, with

$$A^{CP} = \begin{bmatrix} A^P - B^P D^C C^P & B^P C^C \\ -B^C C^P & A^C \end{bmatrix}$$

the system matrix corresponding to the closed-loop interconnection of C and P. If the closed-loop system is internally stable then $\rho(A^{CP}) < 0$. As a result, $\rho(\mathcal{A}) < 0 \Leftrightarrow \rho(A^{CP}) < 1, \rho(A^L) < 1, \rho(A^Q) < 1$.
III. The following shows that $\mathcal{G}(z) = Q(z)(1 - L(z)P(z)S(z))$. First note that $\mathcal{Y}_{k+1}(z) = \mathcal{G}(z)\mathcal{Y}_k(z)$ with $\mathcal{G}(z) = \mathcal{C}(zI - \mathcal{A})^{-1}\mathcal{B}_0 + \mathcal{D}_0$. Using the z-transformed relations (extending the pass length to infinity, similar to the approaches in [2]):

$$\begin{aligned} \mathcal{Y}_{k+1}(z) = f_{k+2}(z) &= Q(z)(f_{k+1}(z) + L(z)e_{k+1}(z)), \\ &= Q(z)(1 - L(z)P(z)S(z))f_{k+1}, \\ &= \mathcal{G}(z)f_{k+1} = \mathcal{G}(z)\mathcal{Y}_k(z), \end{aligned}$$

Hence $\mathcal{G}(z) = Q(z)(1 - L(z)P(z)S(z))$, and $\rho(G(z)) < 1 \Leftrightarrow \rho(Q(z)(1 - L(z)P(z)S(z))) < 1$, with $\rho(Q(z)(1 - L(z)P(z)S(z))) = |Q(z)(1 - L(z)P(z)S(z))|$ since $\mathcal{G}(z) \in \mathbb{C}^{1x1}$. $\square$

Theorem 3 shows that the third condition for stability along the pass in Lemma 2 is equivalent to the well-known frequency-domain ILC convergence condition in [15] for the dLRP (4).

Remark 1. *A standard dLRP such as* (4) *and the notion of stability along the pass require stable* $L(z)$ *and* $Q(z)$*. The dLRP is restricted to a finite-time interval by definition and the infinite-time condition of* (6) *also implies convergence for finite-time if* $L(z)$ *and* $Q(z)$ *are causal (or stable) [15, Theorem 8]. Since the learning update in ILC is typically computed offline, the learning filters are interpreted as a non-causal operator instead of unstable in the ILC context, see e.g., [25, Section 1.5]. The use of causal learning filters is sufficient to illustrate the potential issues with inferential ILC. Further extensions of the dLRP model to allow for a non-causal* L *and* Q *are recently developed in, e.g., [7], [9].*

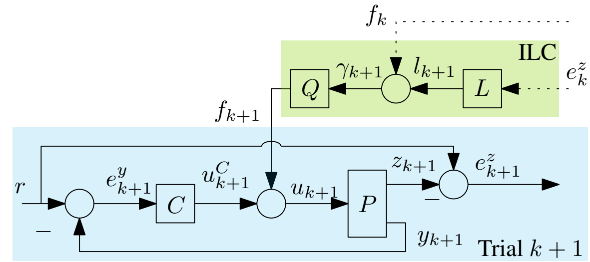

Fig. 2: Parallel inferential ILC structure, with 1-DOF feedback controller.

In the next section, the standard ILC framework is extended to the inferential control situation.

IV. Stability along the pass analysis for inferential ILC

The purpose of this section is to: i) cast inferential ILC structures in a dLRP, ii) analyze an important problematic case where both the $C(z)$ and $L(z)$ include an integrator, and iii) to propose a solution to the problems illustrated with this case, constituting Contribution 2, see Section II.

A. Extension of standard ILC to the inferential setting

As elaborated on in Section II, the explicit distinction between measured variables y_k and performance variables z_k is important for further improving the performance of the controlled system. A typical inferential ILC control structure is presented in Fig. 2, that extends the standard ILC framework of Fig. 1. Alternative inferential ILC configurations are available in, e.g., [4]. The feedback controller uses $e^y_{k+1} = r - y_k$ and the ILC uses $e^z_k = r - z_k$. As mentioned in the introduction, z_k is available after a task. As a first step, it is assumed that $\dim y_k = \dim z_k$. The system P has a single input u_{k+1} and two outputs z_{k+1} and y_{k+1}. A minimal state space realization for P is given by:

$$\begin{aligned} x^P_{k+1}(p+1) &= A^P x^P_{k+1}(p) + B^P u_{k+1}(p), \\ z_{k+1}(p) &= C^{Pz} x^P_{k+1}(p), \\ y_{k+1}(p) &= C^{Py} x^P_{k+1}(p). \end{aligned}$$

The transfer functions from input u_{k+1} to outputs z_{k+1} and y_{k+1} are given by

$$\begin{aligned} P^z(z) &= C^{Pz}(zI - A^P)^{-1}B^P, \\ P^y(z) &= C^{Py}(zI - A^P)^{-1}B^P, \end{aligned}$$

respectively. Realizations of $C(z)$, $L(z)$, and $Q(z)$ are given in (2), where the input to $L(z)$ is changed from e_k to e^z_k. The ILC learning update given by:

$$f_{k+1} = Q\left(f_k + Le^z_k\right).$$

The frequency-domain convergence criterion, identical to the stability along the pass condition 3 in Lemma 2, see Theorem 3, is given by

$$|Q(z)\left(1 - L(z)P^z(z)S^y(z)\right)| < 1, \forall |z| = 1, \tag{8}$$

with $S^y(z) := (1 + C(z)P^y(z))^{-1}$ the sensitivity and $z \in \mathbb{C}$.

B. Inferential ILC as a dLRP

To present the main mechanisms for stability along the pass in inferential ILC, a static $Q(z) = D^Q$ is assumed, with $0 < \rho(D^Q) < 1$, and $D^C = 0$, $D^L = 0$. A realization of the inferential ILC in Fig. 2 is given by the following $\mathcal{A}, \mathcal{B}, \mathcal{B}_0, \mathcal{C}, \mathcal{D}$, and $\mathcal{D}_0$ for the dLRP in (4):

$$\begin{aligned} \mathcal{A} &= \begin{bmatrix} A^P & B^P C^C & 0 \\ -B^C C^{Py} & A^C & 0 \\ -B^L C^{Pz} & 0 & A^L \end{bmatrix}, \; \mathcal{B} = \begin{bmatrix} 0 \\ B^C \\ B^L \end{bmatrix}, \mathcal{B}_0 = \begin{bmatrix} B^P \\ 0 \\ 0 \end{bmatrix}, \\ \mathcal{C} &= \begin{bmatrix} 0 & 0 & D^Q C^L \end{bmatrix}, \qquad \mathcal{D} = \begin{bmatrix} 0 \end{bmatrix}, \quad \mathcal{D}_0 = \begin{bmatrix} D^Q \end{bmatrix}. \end{aligned} \tag{9}$$

with the states defined as:

$$\mathcal{X}_{k+1}(p) = \begin{bmatrix} x^P_{k+1}(p) \\ x^C_{k+1}(p) \\ x^L_{k+1}(p) \end{bmatrix}, \;\; \mathcal{Y}_{k+1}(p) = \begin{bmatrix} f_{k+2}(p) \end{bmatrix}.$$

A part of the results presented in this section is an analysis of the so-called limit-profiles $y_\infty(p) := \lim_{k\to\infty} y_k(p)$ and $x_\infty(p) := \lim_{k\to\infty} x_k(p)$. These limit profiles exist if the dLRP is asymptotically stable. The condition for asymptotic stability is identical to condition 1 in Theorem 3. The limit profiles of (4) are formulated in the following Lemma.

Lemma 4. *Given an asymptotically stable dLRP, i.e., $\rho(\mathcal{D}_0) < 1$, a pass-invariant (or trial invariant) input sequence $r(p)$, and initial conditions $\mathcal{X}_{k+1}(0) = 0$ and $\mathcal{Y}_0(p) = 0$. The 1D state space model that generates the limit profiles $x_\infty(p)$ and $y_\infty(p)$ for $k \to \infty$ is given by:*

$$\begin{aligned} \mathcal{X}_\infty(p+1) &= \mathcal{A}_\infty \mathcal{X}_\infty(p) + \mathcal{B}_\infty r(p), \\ \mathcal{Y}_\infty(p) &= \mathcal{C}_\infty \mathcal{X}_\infty(p) + \mathcal{D}_\infty r(p). \end{aligned}$$

with

$$\begin{aligned} \mathcal{A}_\infty &= \begin{bmatrix} \mathcal{A} + \mathcal{B}_0 (I - \mathcal{D}_0)^{-1} \mathcal{C} \end{bmatrix} = \\ & \begin{bmatrix} A^P & B^P C^C & B^P (I - D^Q)^{-1} D^Q C^L \\ -B^C C^{Py} & A^C & 0 \\ -B^L C^{Pz} & 0 & A^L \end{bmatrix} \\ \mathcal{B}_\infty &= \begin{bmatrix} \mathcal{B} + \mathcal{B}_0 (I - \mathcal{D}_0)^{-1} \mathcal{D} \end{bmatrix} = \begin{bmatrix} 0 & B^C & B^L \end{bmatrix}^T \\ \mathcal{C}_\infty &= (I - \mathcal{D}_0)^{-1} \mathcal{C} = \begin{bmatrix} 0 & 0 & (I - D^Q)^{-1} D^Q C^L \end{bmatrix} \\ \mathcal{D}_\infty &= (I - \mathcal{D}_0)^{-1} \mathcal{D} = \begin{bmatrix} 0 \end{bmatrix} \\ \mathcal{X}_\infty(p) &= \begin{bmatrix} x^P_\infty(p) & x^C_\infty(p) & x^L_\infty(p) \end{bmatrix}^T, \; \mathcal{Y}_\infty(p) = \begin{bmatrix} f_\infty(p) \end{bmatrix}, \end{aligned} \tag{10}$$

for the system matrices in (9).

Proof. Following the approaches in [8, Section 3.1] and [22, Section 2.1] and computing the steady-state value in pass-to-pass direction using $k = k+1 := \infty$ in (4) and rearranging yields (10). □

This is a standard 1D state space model, with as input the reference $r(p)$, and as output the converged pass-profile $f_\infty(p)$ for the control structure in Fig. 2.

C. Application of stability along the pass to inferential ILC

In this section, it is revealed that the case where $C(z)$ has an integrator can be problematic when using the inferential ILC structure in Fig. 2. Integrators in $C(z)$ are present ordinary PID controllers [1] and are also used in high-performance feedback control [13].

The following example case illustrates that condition 2 and 3 for stability along the pass in Theorem 3 cannot be satisfied simultaneously for the structure in Fig. 2, given that certain conditions on C and P are satisfied.

Given a system $P(z)$ with relative degree > 2. Let $\frac{Pz}{Py}(z = 1) = c_0$ with $c_0 \neq 1$ a constant, a stabilizing controller C with an integrator such that $\lim_{z\to 1} C(z)P(z) = \infty$, and a static robustness filter $Q(z) = D^Q$, with $0 < \rho(D^Q) < 1$.

The first condition of stability along the pass, see Theorem 3, is satisfied since $\rho(D^Q) < 1$. The second condition requires $\rho(\mathcal{A}) < 1$, according to Theorem 3 this requires a $L(z)$ with $\rho(A^L) < 1$. To satisfy the the third condition of stability along the pass, the convergence criterion (8) must hold. The learning filter $L(z)$ must include an integrator if $C(z)$ includes an integrator in to satisfy (8). This is based on the observation that $\lim_{z\to 1} P^z(z) S^y(z) = c_0 C(z)^{-1}$. Since $C(z)^{-1}$ has a zero at $z = 1$, the learning filter $L(z)$ must include a pole at $z = 1$, since otherwise $\lim_{z\to 1} c_0 L(z) C(z)^{-1} = \infty$, and (8) can only be satisfied by setting $D^Q = 0$, which is inadmissible since it implies $f_k = 0$.

Concluding this example, if A^C has an eigenvalue $\lambda(A^C) = 1$, then A^L must also have an eigenvalue $\lambda(A^L) = 1$ in order to satisfy the third condition of stability along the pass. It shows that this implies violating the second condition of stability along the pass since in this case $\rho(A^L) = 1$. In the remainder of this section the consequences for including the integrator in $L(z)$ are analyzed.

The following theorem is part of the main result in this paper, contribution 2, in Section II.

Theorem 5. *Given a system $P(z)$ with relative degree $>$ 2. Let $\frac{Pz}{Py}(z = 1) = c_0$ and c_0 a constant, a stabilizing controller C with an integrator (pole at $z = 1$) such that $\lim_{z\to 1} C(z)P(z) = \infty$, and a static robustness filter $Q(z) = D^Q$, with $0 < \rho(D^Q) < 1$. Let $L(z)$ have a pole $z = 1$. The transfer function from $r(z)$ to $f_\infty(z)$ is given by $f_\infty(z) = \mathcal{C}_\infty (zI - \mathcal{A}_\infty)^{-1} \mathcal{B}_\infty r(z)$. With*

$$\lim_{z\to 1} |\mathcal{C}_\infty (zI - \mathcal{A}_\infty)^{-1} \mathcal{B}_\infty| = \infty,$$

if

$$\mathit{Rank} \begin{bmatrix} B^C C^{Py} & B^C \\ B^L C^{Pz} & B^L \end{bmatrix} = 2,$$

and

$$\mathit{Rank} \begin{bmatrix} B^P C^C & B^P (I - D^Q)^{-1} D^Q C^L \\ 0 & (I - D^Q)^{-1} D^Q C^L \end{bmatrix} = 2.$$

Proof. The proof consists of two parts. i) if both A^C and A^L have an eigenvalue $\lambda(A^C) = 1, \lambda(A^L) = 1$ than also $\mathcal{A}_\infty$ has an eigenvalue $\lambda(\mathcal{A}_\infty) = 1$. Suppose that the state space realizations of $C(z)$ and $L(z)$ are in modal form, and hence A^C and A^L are block-diagonal, each with one Jordan block with $\lambda = 1$. Then $\mathcal{A}_\infty$ has a partial block-diagonal structure, with two blocks $\lambda = 1$. Consequently, $\mathcal{A}_\infty - I$ is singular since there are two linearly depended columns. Hence, if $\lambda = 1$ is an eigenvalue of both A^C and A^L, then it also an eigenvalue of $\mathcal{A}_\infty$.

ii) It can be shown that $\lambda(\mathcal{A}_\infty) = 1$ is both controllable and observable using the given rank conditions and the Popov-Belevitch-Hautus observability and controllability tests. If this

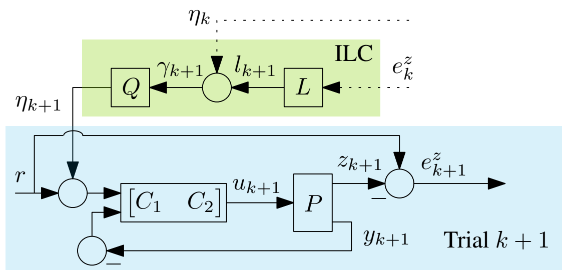

Fig. 3: Serial inferential ILC structure, with 2-DOF feedback controller.

is the case then the transfer function $\mathcal{C}_\infty(zI - \mathcal{A}_\infty)^{-1}\mathcal{B}_\infty$ has a pole $z = 1$. □

The result in this theorem implies that $f_\infty(p)$ increases unbounded if, for example, $r(p) = r$ with r a nonzero constant. This undesired behavior is a result of the violation of condition 2 for stability along the pass in Lemma 2.

Remark 2. *In the non-inferential case with $y_k = z_k$, see Section III, the eigenvalue $\lambda(\mathcal{A}_\infty) = 1$ in* (10) *is not controllable since $C^{Py} = C^{Pz} = C^P$ and therefore*

$$Rank \begin{bmatrix} B^C C^P & B^C \\ B^L C^P & B^L \end{bmatrix} = 1.$$

Consequently, the realization of $Q(z)(1 - PSL(z))$ using the structure in Fig. 1 is not a minimal implementation if both $C(z)$ and $L(z)$ include an integrator. The solution to this case is outside the scope of this paper and will be published elsewhere.

In the next section, an alternative inferential ILC structure is proposed, that effectively deals with the problem of unbounded command signals, by transitioning from a parallel to a serial ILC structure.

D. An inferential ILC solution

In the previous section, it was shown that using a parallel ILC structure in conjunction with feedback as in Fig. 2 leads to the undesired characteristic of an infinite gain from $r(p)$ to $f(p)$ at the zero frequency if both $C(z)$ and $L(z)$ include an integrator and a static $Q(z) = D^Q$ is used. A solution is to transition from a parallel ILC structure such as in Fig. 2 to a serial ILC structure, and using a 2-DOF feedback controller, see [17], in order to remove the limitation $\dim y = \dim z$. This proposed structure is presented in Fig. 3. The ILC command signal is added to the reference of the feedback loop, instead of the feedforward.

Since this is a serial ILC structure, this configuration is encompassed in the ILC framework elaborated on in Section III by setting $C(z) = 0$ and setting $P(z) := T^z(z)$ with $T^z(z) = P^z C_1(z)(1 + C_2 P^y(z))^{-1}$. The frequency-domain ILC convergence criterion, or stability along the pass condition 3, see Lemma 2 is given by:

$$|Q(z)(1 - L(z)T^z(z)| < 1, \forall |z| = 1, z \in \mathbb{C}. \quad (11)$$

Using this framework, stability along the pass can be obtained, even if A^{C_2} has an eigenvalue $\lambda(A^{C_2}) = 1$. Condition 1 of Theorem 3 can be satisfied by designing a $Q(z)$ with $\rho(D^Q) < 1$. Condition 2 is satisfied, if $C_2(z)$ is stabilizing controller and $L(z)$ is stable. Condition 3 is satisfied by using an suitable approximation $L(z) \approx T^z(z)^{-1}$, not violating condition 2, and introducing $Q(z)$ if necessary for robustness reasons to satisfy convergence condition (11).

The problem illustrated in Section IV-C does not occur since the three conditions for stability along the pass in Theorem 3 can be satisfied, even if C includes integrators.

V. Simulation results

The derived results in Section IV-C and Section IV-D are illustrated by means of a simulation. The structure in Fig. 2 is compared with the structure presented in Fig. 3 in a case study on a model of a medium positioning drive in a wide-format printer.

1) System model: The system P is a model of a medium positioning drive in a wide-format printer, see [3]. The feedback controller $C_1(z) = C_2(z) = C(z)$ is given, and consists of a PID-controller with a first order low-pass filter. The Bode diagrams of $P^z(z)$, $P^y(z)$ and $C(z)$ are presented in Fig. 4. For this system, $\lim_{z\to 1} \frac{P^z}{Py} = 1.028$, hence identical conditions as in the problematic example case are present, see Section IV-C.

2) ILC design: For both structures, the learning filters $L(z)$ are computed by using the inverse-model approximation in [24], where the non-causal time-shift is set to 0. The robustness filter $Q(z) = 0.1$.

The learning filter for the structure in Fig. 2 includes an integrator. Consequently, the ILC algorithm can not be stable along the pass since condition 2 in Theorem 3 is violated. The frequency-domain convergence condition 3, see Theorem 3, is satisfied, hence Theorem 5 applies to this case and it is expected that f_k grows unbounded with the given $r(p)$.

The structure in Fig. 3 is stable along the pass for this case with the given L and Q.

3) Results: The simulations are invoked using the reference $r(p)$, that is a smoothed step in position from 0 to 0.1 m in 0.5 s time. The converged command signals are presented in Fig. 5a and Fig. 5b, for the parallel inferential ILC structure, and 2-DOF serial ILC structure, respectively. The results demonstrate that using the structure in Fig. 2 can lead to unbounded growth of the command signals of the ILC and the feedback controller, with opposite sign, as is seen in Fig. 5a, this supports the result in Theorem 5. The structure of Fig. 5b does not suffer from such a phenomenon, since it is stable along the pass. The resulting input $u_\infty(p)$ of the system P is identical for both structures.

VI. Conclusion

This paper features an in-depth analysis of inferential ILC. It is shown that directly casting feedback-feedforward structures to the inferential setting can lead to configurations that are not stable in a 2D systems setting.

This aspect is analyzed in detail by casting the time-trial dynamics into a discrete linear repetitive process, a class of 2D systems. In order to facilitate the analysis of the inferential control structure, the 2D stability notion of stability along the pass is translated to conditions on the ILC algorithm, feedback controller, and process.

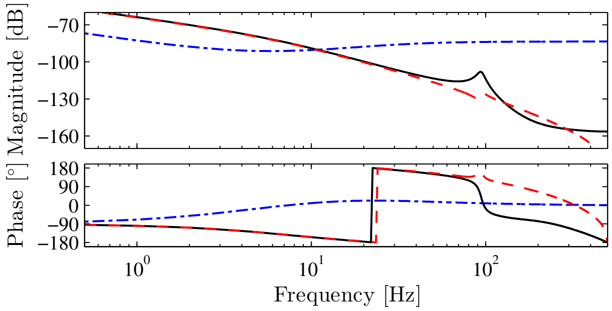

Fig. 4: Frequency response functions of $P^z(z)$ (black solid), $P^y(z)$ (dashed red), and $C(z) \cdot 10^{-9}$ (dashed-dotted blue).

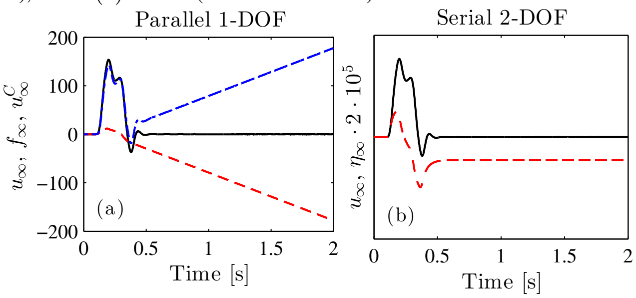

Fig. 5: Left (a), converged command signals $u_\infty(p)$ (black solid), $f_\infty(p)$ (dashed red), and $u_\infty^C(p)$ (dashed-dotted blue). The parallel inferential ILC structure is not stable along the pass: the command signals of the feedback controller and the ILC grow unbounded with opposite sign, see Theorem 5, due to the interplay of $C(z)$ with the ILC.
Right (b), converged command signals $u_\infty(p)$ (black solid) and $\eta_\infty(p)$ (dashed red). The serial inferential ILC structure is stable along the pass and does not suffer from the phenomenon in (a), see Section IV-D.

In case the feedback controller and learning filter have an integrator, that the state space system that generates the converged feedforward and error signals also includes this integrator. Analysis reveals that this eigenvalue is observable and controllable in the case of inferential ILC with a parallel structure. As such, the ILC command signal increases unbounded if the applied reference is constant and nonzero. A solution to this problem is presented and relies on changing the controller structure from a parallel to a serial configuration. A simulation example on a medium positioning drive of a wide-format printer is included to illustrate these conclusions.

Currently, inferential ILC is being implemented on the medium positioning drive in an experiment, see [3]. Ongoing research is towards multi-degree-of-freedom inferential ILC structures and inter-sample behavior.

Acknowledgment

The authors would like to acknowledge the fruitful discussions with the late professor Okko Bosgra and Sjirk Koekebakker that have significantly contributed to the results.

This work is supported by Océ Technologies, P.O. Box 101, 5900 MA Venlo, The Netherlands. This work is also supported by the Innovational Research Incentives Scheme under the VENI grant “Precision Motion: Beyond the Nanometer” (no. 13073) awarded by NWO (The Netherlands Organisation for Scientific Research) and STW (Dutch Science Foundation).

References

[1] K. Åström and T. Hägglund, *PID Controllers: Theory, Design, and Tuning*. The Instrumentation, Systems, and Automation Society, 1995.

[2] F. Boland and D. Owens, “Linear Multipass Processes: a Two-dimensional Interpretation,” *Proc. IEE*, vol. 127, pp. 189–193, 1980.

[3] J. Bolder, T. Oomen, S. Koekebakker, and M. Steinbuch, “Using iterative learning control with basis functions to compensate medium deformation in a wide-format inkjet printer,” *In press, IFAC Mechatronics*. [Online]. Available: http://dx.doi.org/10.1016/j.mechatronics.2014.07.003

[4] J. Bolder, T. Oomen, and M. Steinbuch, “On Inferential Iterative Learning Control: with example to a printing system,” *Proc. Americ. Contr. Conf., Portland, OR, USA*, pp. 1827–1832, 2014.

[5] D. Bristow, M. Tharayil, and A. Alleyne, “A Survey of Iterative Learning Control: a Learning-based Method for High-performance Tracking Control,” *IEEE Contr. Syst. Mag.*, vol. 26, pp. 96–114, 2006.

[6] Y. Chen, K. Moore, J. Yu, and T. Zhang, “Iterative Learning Control and Repetitive Control in Hard Disk Drive Industry - A Tutorial,” *Int. J. Adapt. Contr. Sign. Proc.*, vol. 23, pp. 325–343, 2008.

[7] B. Cichy, K. Galkowski, and E. Rogers, “2D Systems Based Robust Iterative Learning Control using Noncausal Finite-time Interval Data,” *Syst. Contr. Lett.*, vol. 64, pp. 36–42, 2014.

[8] J. Edwards and D. Owens, *Analysis and Control of Multipass Processes*. Research Studies Press, 1982.

[9] K. Galkowski, B. Cichy, E. Rogers, and J. Lam, “Stabilization of a class of uncertain “wave” discrete linear repetitive processes,” *Proc. Conf. Dec. Contr., San Diego, CA, USA*, pp. 1435–1440, 2006.

[10] D. Gorinevsky, “Loop Shaping for Iterative Control of Batch Processes,” *IEEE Contr. Syst. Mag.*, vol. 22, pp. 55–65, 2002.

[11] D. Hoelzle, A. Johnson, and A. Alleyne, “Bumpless Transfer Filter for Exogeneous Feedforward Signals,” *IEEE Trans. Contr. Syst. Techn.*, vol. 22, pp. 1581–1588, 2014.

[12] R. Longman and C.-P. Lo, “Generalized Holds, Ripple Attenuation, and Tracking Additional Outputs in Learning Control,” *J. Guid., Contr., Dyn.*, vol. 20, pp. 1207–1214, 1997.

[13] D. McFarlane and K. Glover, *Robust Controller Design Using Normalized Coprime Factor Plant Descriptions*. Springer-Verlag, 1990.

[14] S. Mishra, U. Topcu, and M. Tomizuka, “Optimization-Based Constrained Iterative Learning Control,” *IEEE Trans. Contr. Syst. Techn.*, vol. 19, pp. 1613–1621, 2011.

[15] M. Norrlöf and S. Gunnarsson, “Time and Frequency Domain Convergence Properties in Iterative Learning Control,” *Int. J. Contr.*, vol. 75, pp. 1114–1126, 2002.

[16] T. Oomen, O. Bosgra, and M. van de Wal, “Identification for Robust Inferential Control,” *In Proc. Joint Conference on Decision and Control and Chinese Control Conference, Shanghai, China*, pp. 2581–2586, 2009.

[17] T. Oomen, E. Grassens, F. Hendriks, R. van Herpen, and O. Bosgra, “Inferential Motion Control: Identification and Robust Control with Unmeasured Performance Variables,” *Proc. Conf. Dec. Contr. and European Control Conference, Orlando, FL*, pp. 964–969, 2011.

[18] T. Oomen, R. van Herpen, S. Quist, M. van de Wal, O. Bosgra, and M. Steinbuch, “Connecting System Identification and Robust Control for Next-Generation Motion Control of a Wafer Stage,” *IEEE Trans. Contr. Syst. Techn.*, vol. 22, pp. 102–118, 2014.

[19] G. Parmar, K. Barton, and S. Awtar, “Large Dynamic Range Nanopositioning Using Iterative Learning Control,” *Prec. Eng.*, vol. 38, pp. 48–56, 2014.

[20] J. Parrish and C. Brosilow, “Inferential Control Applications,” *Automatica*, vol. 21, no. 5, pp. 527–538, 1985.

[21] W. Paszke, R. Merry, and R. van de Molengraft, “Iterative Learning Control by Two-Dimensional System Theory applied to a Motion System,” *Proc. Americ. Contr. Conf., New York City, USA*, pp. 5484–5489, 2007.

[22] E. Rogers, K. Galkowski, and D. Owens, *Control Systems Theory and Applications for Linear Repetitive Processes*. Springer-Verlag, 2007.

[23] A. Schoellig, F. Mueller, and R. D'Andrea, “Optimization-Based Iterative Learning for Precise Quadrocopter Trajectory Tracking,” *Autonomous Robots*, vol. 33, pp. 103–127, 2012.

[24] M. Tomizuka, “Zero Phase Error Tracking Algorithm for Digital Control,” *J. Dyn. Syst., Meas., and Contr.*, vol. 109, pp. 65–68, 1987.

[25] G. Vinnicombe, *Uncertainty and Feedback: $\mathcal{H}_\infty$ loop-shaping and the ν-gap metric*. Imperial College Press, London, UK, 2001.

[26] J. Wallén, M. Norrlöf, and S. Gunnarsson, “A Framework for Analysis of Observer-based ILC,” *Asian Journal of Control*, vol. 13, pp. 3–14, 2011.